Unravelling Surfactant Partitioning: Part 2 – Experimental Study of Multi-component Surfactant Partitioning Responses and their Influence on Inhibition Performance

Richard Barker, Joshua Owen,
Raeesa Bhamji, Jeanine
Williams, Amber Sykes, Yasmin
Hayatgheib, Dilshad Shaikhah,
Richard C. Woollam,
Faculty of Engineering and
Physical Sciences
University of Leeds
Woodhouse Lane
Leeds, LS2 9JT
United Kingdom

William H. Durnie
bp Australia
240 St. Georges Terrace
Perth
Western Australia

Mariana C. Folena, Abubaker
Abdelmagid, Hanan Farhat
The Corrosion Center
Qatar Environment & Energy
Research Institute
Hamad Bin Khalifa University
Doha
34110
Qatar

ABSTRACT

In Part 1 of this two-part paper, a predictive model for multi-component partitioning was developed based on knowledge of individual component micellization and partitioning characteristics. In Part 2, the model's validity is assessed through comparison with experimental partitioning data for an 1 wt.% NaCl brine:toluene system containing mixtures of two benzylammonium chloride corrosion inhibitors (BAC- C_{12} and BAC- C_{16}).

Following model validation, the implications of the experimental partitioning behavior on corrosion inhibition performance are examined via rotating cylinder electrode (RCE) experiments. Through selected experiments, the important role of each of the two surfactants and their relative molar concentration in influencing overall corrosion inhibition performance is examined. While BAC-C₁₂ exhibited poor inhibition in isolation, when combined with BAC-C₁₆ at specific molar ratios, BAC-C₁₂ played a crucial role in retaining the longer chain surfactant in the aqueous phase. This response enabled BAC-C₁₆ (the more effective surfactant corrosion inhibitor) to work synergistically with BAC-C₁₂ to suppress carbon steel corrosion more effectively than the two components alone under these particular conditions.

Key words: CO₂ Corrosion, partitioning, corrosion inhibitors, micelle, CMC, salinity.

INTRODUCTION

In Part 1 of this two-part paper, an idealized model was developed to understand the distribution behavior of multi-component surfactants in oil-water systems. In terms of physical property inputs, the model requires the aqueous critical micelle concentration (CMC) of each pure surfactant, oil CMC of each pure surfactant, total mixed surfactant concentration and the partition coefficient of each individual surfactant. Additional system input properties include the water and oil volume ratio and the mixed molar ratio of surfactant added based on the total fluid.

In terms of approach, the model determines the respective molar ratios of mixed surfactants in each phase based on each surfactants individual partition coefficient, predicting their evolution in each phase as a function of total surfactant loading. The model then uses the pure surfactant aqueous and oil CMC values, along with their respective molar ratios within each phase to determine the oil/aqueous mixture CMCs, and ultimately, the total concentration and associated phase in which micellization occurs i.e. the 'break point' at which the distribution coefficient begins to vary from that of the partition coefficient.

In Part 1, a set of experimental data relating to pure components from previous studies (shown in Table 1) was incorporated into the model for dimethyldodecylbenzylammonium chloride and dimethylhexadecylbenzylammonium chloride (BAC-C₁₂ and BAC-C₁₆, respectively).^{1, 2}

Table 1: Input parameters associated with surfactants for oil-water distribution model for a toluene-1 wt.% NaCl solution at 50°C

Parameter	BAC-C ₁₂	BAC-C ₁₆	
$P_{w/o,i}$	36	0.16	
$CMC_{w,i}$	1409 µM	23 µM	
$CMC_{o,i}$	79 µM	120 µM	

The effect of surfactant concentrations, relative surfactant molar ratios based on total fluid volume, and water cut on partitioning/distribution behavior was examined in Part 1. In Part 2, the model's capabilities in predicting single and multi-component partitioning responses is assessed. The response is combined with experimental corrosion data to understand the implications on corrosion inhibition performance for these two surfactant combinations through specific rotating cylinder electrode (RCE) experiments.

EXPERIMENTAL PROCEDURE

The two surfactants chosen in this study were dimethylbenzyldodecylammonium chloride (BAC-C₁₂) and dimethylbenzylhexadecylammonium chloride (BAC-C₁₆), sourced from Sigma Aldrich with >99% purity.

Partitioning Experiments

All partitioning tests were performed at 50°C using toluene as the hydrocarbon phase, with the aqueous phase consisting of pH 4, 1 wt.% Sodium Chloride (NaCl) solution. All tests were conducted with a 50:50 volume fraction of aqueous to hydrocarbon phase. Prior to each test, the brine was prepared by mixing analytical grade NaCl with deionized water until dissolved. The brine pH was subsequently adjusted to pH 4 using dilute hydrochloric acid. The hydrocarbon phase consisted of HPLC-grade toluene. Both the hydrocarbon and brine phase were pre-saturated by adding a sufficient quantity of each to the other to maintain a two-phase system, leaving overnight at room temperature to ensure equilibrium. Pre-saturated fluids were used for all partitioning tests. Stock solutions of BAC-C₁₂, BAC-C₁₆ and their mixtures, with known, precise concentrations (1,000, 10,000 and 100,000 mg/L) were prepared in methanol and were used to achieve the desired concentration of inhibitor in each vial whilst maintaining accuracy. Equal known volumes (15 ml) of the pre-saturated aqueous and toluene phases were added to a 40 ml glass vial. A known volume of stock solution, calculated to achieve the desired inhibitor concentration (either pure of mixed) was added to the vial. Concentration was calculated based on the total volume of both

fluids. The concentrations, assessed based on the total volume, ranged from 2.5 to 500 mg/L (ppm), depending on the experiment, but are expressed as molar concentrations throughout the paper.

Each vial was sealed, gently agitated and placed in a water bath at 50°C for a minimum of 24 h. If no emulsion was detected at the interface, the toluene and brine phases were extracted using a syringe and needle while still at test temperature. Concentrations at which a persistent third-phase developed were not analyzed, though these were typically at concentrations close to an order of magnitude greater than were the 'break-points' in partitioning responses were observed.

HPLC-MS Analysis

Preparation of Standards

Standards for the BAC- C_{12} and BAC- C_{16} (0.1-10 mg/L) were prepared in brine as well as toluene for calibration purposes. The standards were processed in the same way as each phase from the partitioning experiments.

Solid Phase Extraction of Brine Fractions

The brine standards and fractions obtained from each of the partitioning experiments were processed by solid phase extraction (SPE). Waters Oasis HLB 6cc (150mg) extraction cartridges were used to extract the model compounds from the brine samples into methanol with 0.1% (v/v) formic acid for analysis on LC-MS. The cartridges were placed on an SPE vacuum manifold, solvated with 3 mL methanol and then flushed with 3 mL of deionized water. The sample (5 mL) was loaded onto the cartridge, and eluted with 3 mL of deionized water. The cartridge was allowed to run dry under vacuum. The model compounds were then eluted from the cartridge using 5 mL of methanol with 0.1% (v/v) formic acid into a 5 mL volumetric flask.

Preparation of Toluene Fraction for Analysis

The toluene standards and fractions were diluted 1:3 with 0.1% (v/v) formic acid in methanol before being analyzed by LC-MS.

HPLC Methodology for Partitioning Analysis

Liquid chromatography with mass spectrometry (LC-MS) was used to determine the concentrations of the compounds in the two phases of the partitioning experiments. An Agilent 1290 Infinity II HPLC system was connected to an Agilent 6120B single quadrupole mass spectrometer with an Electrospray Ionization source. The column (Avantor ACE 3 C18, 3 μ m, 100 x 3 mm) was kept at 40°C, and a flow rate of 0.5 mL/min, with 0.1% formic acid and 5 mM ammonium formate in water as solvent A, and 0.1% formic acid in methanol as solvent B. The gradient program started with 50% of solvent A for 0.5 minutes, and then ramped up to 100% of solvent B over 10 minutes. The 100% of solvent B was maintained for another 5 minutes, and returned to initial conditions (50% solvent A) over 2 minutes. The prepared samples were injected at a volume of 1 μ L. The electrospray ionization source was run in the positive mode, with the product ion of 304 and 360.7 m/z and 304 m/z used for selected ion monitoring (SIM) of BAC-C₁₂ and BAC-C₁₆, respectively.

Aqueous CMC analysis

Solution Preparation

The aqueous CMC was measured using a spectrophotometric method involving the lipophilic dye Nile Red; this method was selected as the dye probes the micelles directly rather than relying on surface tension as a proxy for micelle detection. The test solution was prepared from a concentrated inhibitor stock solution with typically ten times greater concentration than the highest sample concentration evaluated in each mixture experiment. Given the reversible nature of micelle formation, this is a valid approach, providing that the various test solutions formulated at lower concentrations were afforded enough time to re-equilibrate.

To achieve the desired concentration, each sample was prepared by weighing out a minimum required mass of surfactant in a 250 mL beaker, dissolving in the appropriate volume of 1 wt.% NaCl brine solution

at pH 4 (set using 1M hydrochloric acid). The inhibitor was dissolved in the solution at 50°C using a magnetic stirrer to ensure full dissolution. The concentrated stock solution was then combined with either the 1 wt.% NaCl solution at pH 4 in different ratios and mixed thoroughly for ~15 minutes to achieve ~14-20 samples with concentrations spanning two to three orders of magnitude. A 7 mL sample was taken from each of the brine solutions and placed into a sealed vial. A sample with no surfactant was collected in order to initially 'zero' the spectrophotometer during measurements. All sealed vials were then stored in a water bath at 50°C for ~1 h.

Nile Red Addition and Incubation

Nile Red dye was used to identify the absence or presence of micelles in each collected sample. Nile Red powder was dissolved in methanol to produce a 1000 μ M concentration dye. 70 μ L of dye was pipetted into each 7 mL vial (with the exception of the 'zero' sample). After addition of the dye, each vial was then shaken vigorously for >1 minutes and placed back in the water bath. After Nile Red had been added to the final sample, the vials were left to incubate in the water bath for 30 minutes before beginning measurements in the spectrophotometer. One minute was left between Nile Red additions into each sample to account for the time between spectrophotometer readings, to ensure consistent incubation times for every sample.

Spectrophotometer Readings

A DR3900^[1] Laboratory Spectrophotometer was used to determine the absorbance spectra across the various concentrations of BAC-C₁₂ and BAC-C₁₆ in 1 wt.% NaCl brine. After 30 minutes incubation, the spectrophotometer readings began with the zero sample (containing no inhibitor) to calibrate/zero the spectrophotometer. The readings for all the inhibitor samples were then carried out in order of increasing concentration. Samples were poured into a cuvette and placed in the spectrophotometer which measured the absorbance of each sample across the visible light spectrum from 350-800 nm wavelength. A higher concentration of micelles in a sample would result in a greater aggregation of Nile Red. This effectively produces a greater intensity of solution colour that would absorb more light and result in a higher peak absorbance measurement. Peak absorbance was typically observed between 560-590 nm wavelengths.

Data Analysis / Aqueous CMC Determination

The absorbance spectra for each sample was transferred from the spectrophotometer to a PC. The peak absorbance of each sample was recorded in the range 560-590 nm from each spectra and plotted against sample concentration on a logarithmic scale. Two distinct trends were apparent in the plot. At low, pre-CMC concentrations, absorbance was relatively unchanged with increasing concentration, up to a point. Further increase in concentration above CMC resulted in absorbance increasing dramatically. Linear trend lines were fitted to these pre-CMC and post-CMC regions and the point at which they intersected was deemed to be the CMC of that inhibitor. Each CMC analysis was repeated a minimum of 3 times.

Corrosion Rate Determination

Material

X65 (UNS K03014) carbon steel coupons were used as the working electrodes as part of a rotating cylinder electrode (RCE) setup. The chemical composition of the X65 carbon steel is provided in Table 2, with the microstructure consisting of ferrite and pearlite phases. Prior to the start of each experiment, the surface of the electrode was wet-ground with silicon carbide paper up to 600-grit, degreased with acetone, rinsed with distilled water and dried with compressed air before being placed in the test solution.

Table 2
Elemental composition of X65 carbon steel (in wt.%)

С	Mn	Ni	Nb	Мо	Si	V	Р	S	Fe
0.15	1.422	0.09	0.054	0.17	0.22	0.06	0.025	0.002	Bal.

Experimental Setup

Experiments were conducted using an RCE at 1000 rpm in 1 L of CO₂-saturated 1 wt.% NaCl solution at 50°C and pH ~4 across a range of selected inhibitor concentrations, with use of a 25 mm length magnetic stirrer in the bottom of the vessel, rotating at 500 rpm to ensure thorough mixing of the surfactant within the test solution. Prior to each experiment the test solution was saturated with CO₂ gas for a minimum of 12 h at room temperature before heating to the desired test temperature. All tests were carried out at atmospheric pressure. A standard three-electrode cell configuration was used within the RCE in order to conduct CO₂ corrosion experiments with the X65 carbon steel coupon serving as the working electrode, a silver/silver chloride (Ag/AgCl) reference electrode and a platinum counter electrode. A 15 minute precorrosion period was used prior to inhibitor addition to the test solution. All inhibitors were injected into the test solution using a pipette, after pre-dissolving in a known quantity of methanol.

Corrosion Rate Measurement

Electrochemical measurements were performed using an Ivium^[2] compactstat potentiostat. Linear Polarization Resistance (LPR) measurements were performed for each inhibitor concentration trialed. Measurements were performed every 2-3 minutes by scanning from -5 mV vs. open circuit potential (OCP) to +5 mV vs. OCP at a scan rate of 0.25 mV/s. The corrosion rate at each instance in time was obtained from the measured polarization resistance using a Stern-Geary coefficient of 26 mV.

RESULTS

Pure Component Distribution Responses

The distribution responses of pure BAC- C_{12} and BAC- C_{16} in the 50:50 toluene-1 wt.% brine system at 50°C is provided in Figure 1, noting that the lines on the graph are trend lines, and not those predicted by the distribution model itself. As expected from the literature, ^{2,3} the equilibrated concentrations of each pure surfactant varies linearly within each phase as total concentration increases, up to the point of micellization. Prior to micellization, the concentration in the oil and aqueous phase vary proportionally with one another. This proportional response enables the partition coefficients of the pure surfactants to be determined, providing the physical inputs into the multi-component distribution model. The experimental partition coefficients ($P_{\text{W/o}}$) in Figure 1 were determined as 36 and 0.16, for BAC- C_{12} and BAC- C_{16} , respectively.

Though the BAC- C_{12} oil CMC, and the BAC- C_{16} aqueous CMC can both be theoretically determined from the 'break-point' in Figures 1(a) and (b), respectively, as illustrated, Nile Red and Dynamic Light Scattering (DLS)/partitioning data from literature² were used to determine/validate the majority of model input parameters. The purpose behind this was to two-fold:

- i. To validate the theory that micellization is indeed responsible for the presence and location of the 'break-point'.
- ii. Figures 1(a) and (b) do not permit determination of BAC-C₁₂ aqueous CMC and BAC-C₁₆ oil CMC in toluene, which are also required model inputs.

_

^[2] Trade Name

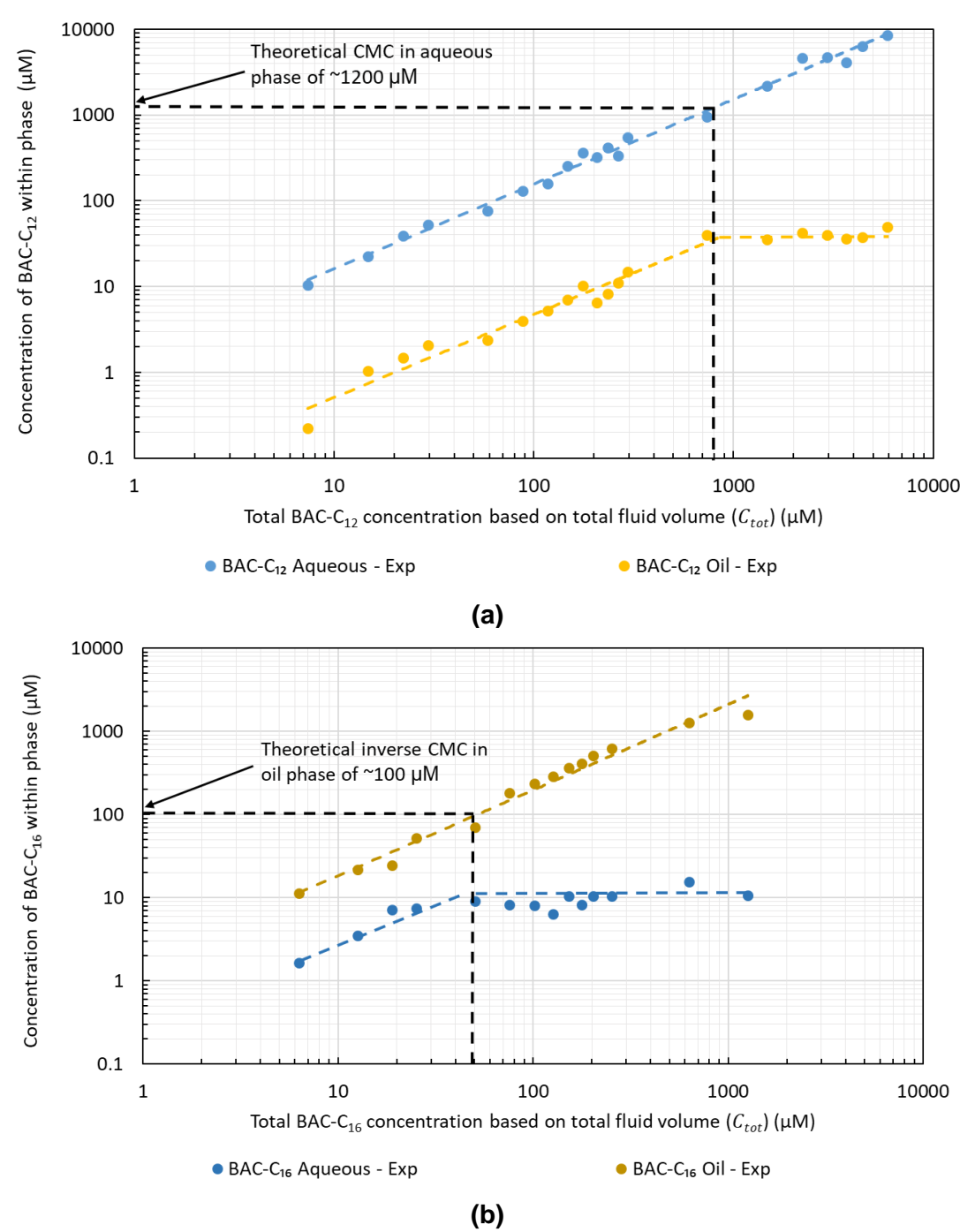


Figure 1: Partitioning data for (a) BAC-C₁₂ and (b) BAC-C₁₆ between 1 wt.% NaCl brine and toluene. Note that the dashed lines represent trend lines, not predictions generated by the oilwater distribution model.

Figure 2(a) provides an example of the outputs generated from the use of the Nile Red method to determine the aqueous CMC of BAC- C_{12} . The determined values of 1409 μ M for the aqueous CMC of BAC- C_{12} aligns well with the values predicted from the partitioning responses in Figure 1(a). Furthermore, the values of 120 μ M determined by Zhu and Free² using DLS measurement for the oil reverse CMC of BAC- C_{16} in toluene align well with the values determined from the partitioning responses in Figure 1(b), reinforcing the theory that the observed break-points are associated with micellization. The Nile Red method was also used to determine aqueous CMC of BAC- C_{16} in 1 wt.% NaCl (23 μ M, as shown in Figure 2(b)), whilst the reverse CMC of BAC- C_{12} in toluene (79 μ M) was determined as part of a separate partitioning study using identical chemistries.

The partition coefficient measurements from Figure 1, combined with the CMC values determined using the various measurement techniques provides the necessary physical inputs for the distribution model.

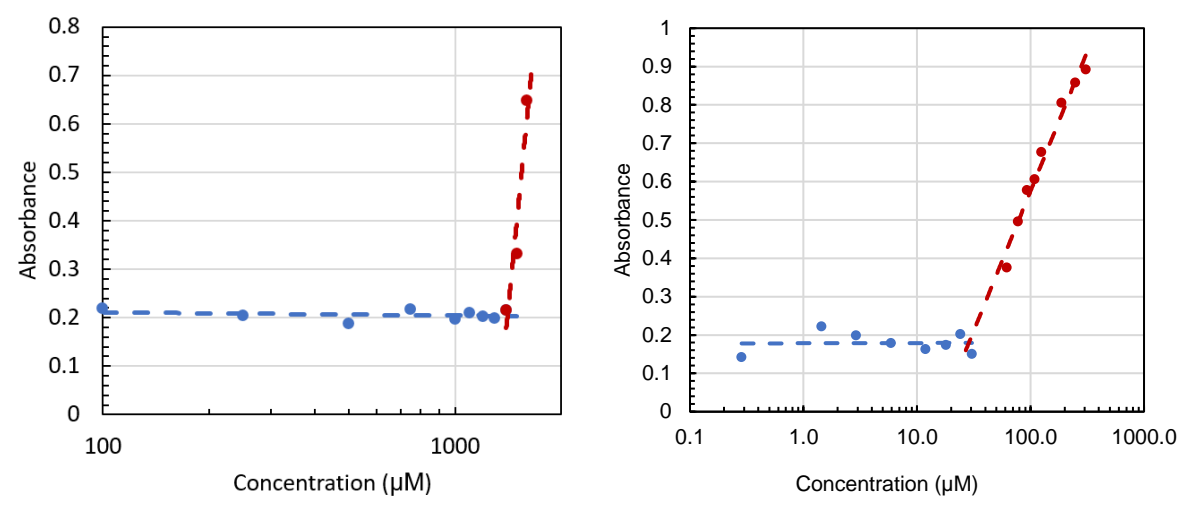


Figure 2: Nile red test results to determine aqueous CMC of (a) BAC-C₁₂ and (b) BAC-C₁₆ in a 1 wt.% NaCl solution.

Multi-component Partitioning

Part 1 examined the behavior of the distribution model over variations in surfactant mixture composition. Two particular molar ratios between BAC-C₁₂ and BAC-C₁₆ are brought forward to this paper as a means of validating the distribution model and understanding how the variation in composition influences corrosion inhibition in the aqueous phase. These compositions relate to 1:1 and 4:1 ratios of BAC-C₁₂ to BAC-C₁₆, with the justification being that switching between these compositions imposed a reversal in the partitioning response of the surfactant components, with the 1:1 mixture favoring micellization in the toluene phase, and the 4:1 mixture resulting in formation of micelles in the aqueous phase.

Regarding the 1:1 mixture of BAC-C₁₂ to BAC-C₁₆, Figure 3 illustrates the predicted distribution response of each of the two surfactants within both the toluene and 1 wt.% NaCl brine phases. The model prediction is represented by the solid lines, whilst the experimental partitioning data determined using HPLC-MS is represented using the individual markers. Figure 3 illustrates there is a strong agreement between the model prediction and the experimental partitioning data under the conditions evaluated. The model is able to accurately predict the preferential formation of mixed micelles in the toluene phase, as well as the total concentration at which this occurs.

Figure 4 shows the effect of changing the molar ratio from 1:1 to 4:1 for BAC-C₁₂ to BAC-C₁₆, which results in a reversal of the partitioning behavior. Again, the model successfully captures the resulting distribution response. The important observation in Figure 4 is that the concentration of both surfactants in the aqueous phase continues to increase with total concentration beyond the break-point.

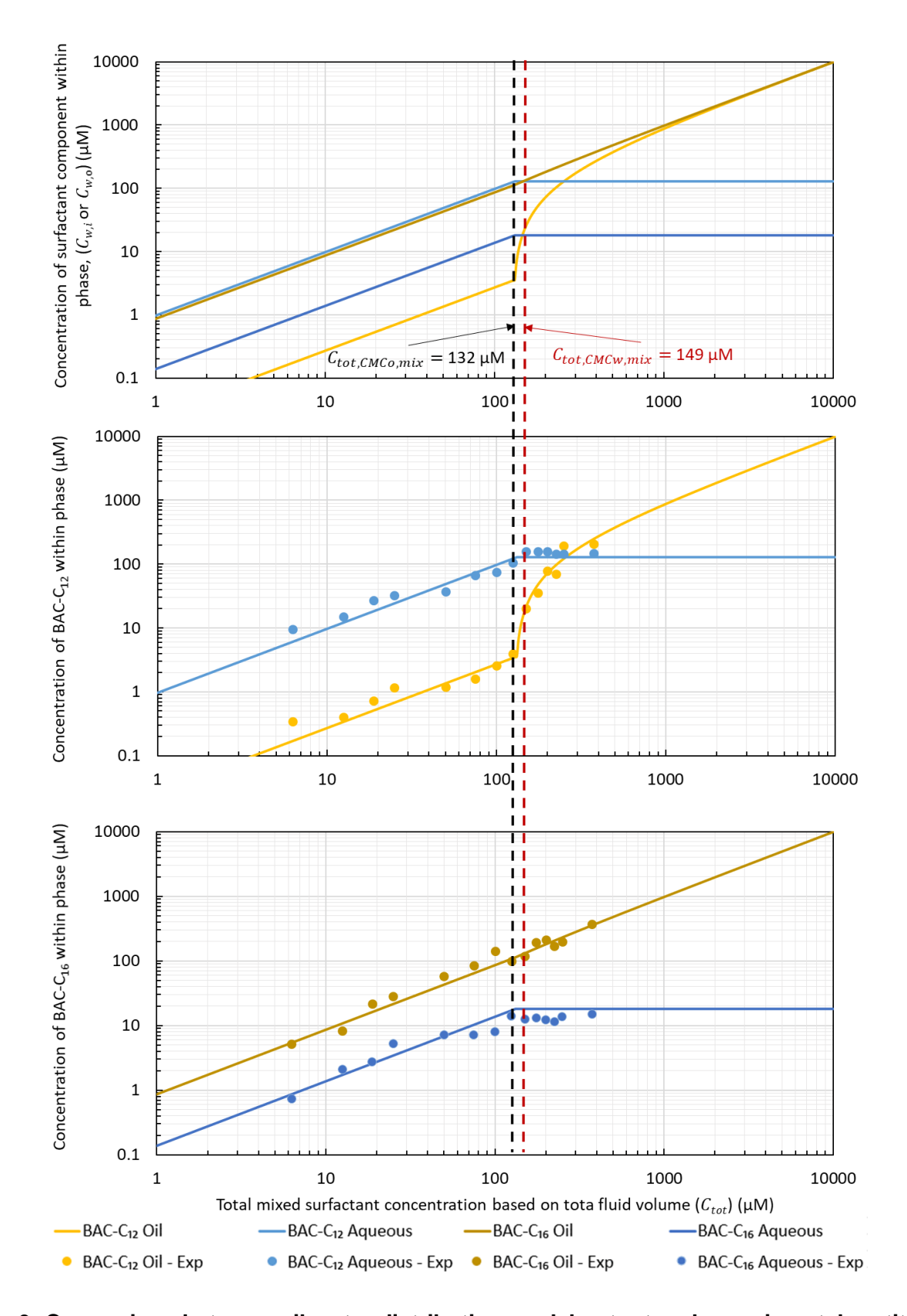


Figure 3: Comparison between oil-water distribution model output and experimental partitioning data for a 50-50 toluene-1 wt.% brine system at surfactant mixture molar ratio of 1:1 for BAC-C₁₂ to BAC-C₁₆. Top: Model prediction; Middle: Model prediction and experimental data for BAC-C₁₂; Bottom: Model prediction and experimental data for BAC-C₁₆.

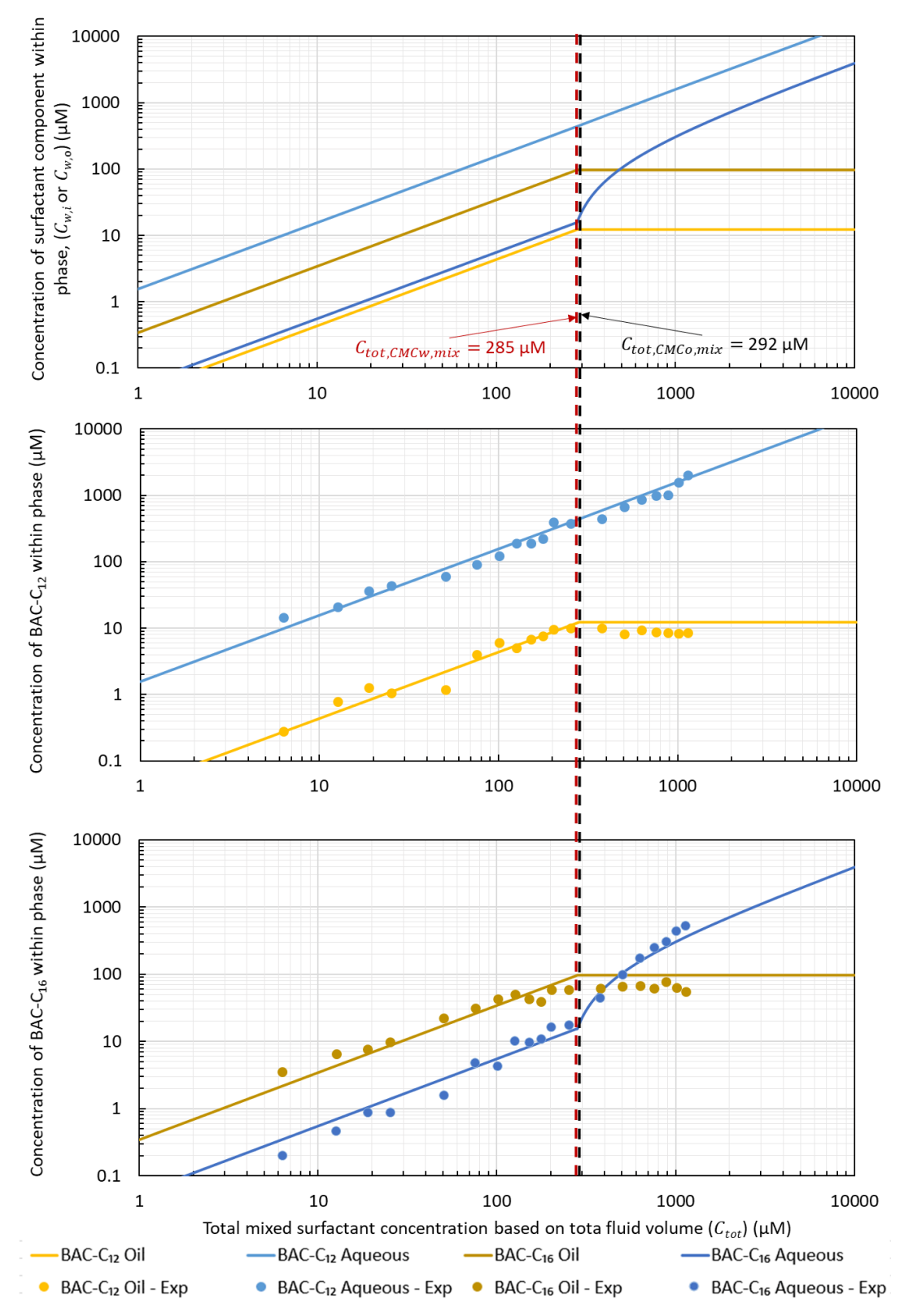


Figure 4: Comparison between oil-water distribution model output and experimental partitioning data for a 50-50 toluene-1 wt.% brine system at surfactant mixture molar ratio of 4:1 for BAC-C₁₂ to BAC-C₁₆. Top: Model prediction; Middle: Model prediction and experimental data for BAC-C₁₂; Bottom: Model prediction and experimental data for BAC-C₁₆.

Influence of Single Component Partitioning on Corrosion Inhibition Performance

Revisiting Figures 1(a) and (b), it is clear that BAC- C_{12} and BAC- C_{16} exhibit very different partitioning responses, with BAC- C_{12} forming micelles and preferentially distributing in the aqueous phase, whilst BAC- C_{16} preferentially distributes and forms micelles in the toluene phase. The question from a corrosion management perspective relates to the implications of the partitioning response on corrosion inhibition performance for BAC- C_{12} and BAC- C_{16} .

Figure 5 provides an example corrosion rate vs time response for X65 steel after addition of 100 μ M BAC-C₁₆ after 15 minutes of pre-corrosion. The environment under which BAC-C₁₆ is evaluated correspond to those of the aqueous phase studied in the partitioning experiments (i.e. 1 wt.% NaCl brine at pH 4, 50°C) with a rotation of 1000 rpm set for the RCE. From Figure 5, it is possible to estimate a value of steady-state surface coverage using Eq. 1:

$$\theta = \left(1 - \frac{V_i}{V_{un}}\right)$$
 Eq. 1

where V_i is the minimum corrosion rate observed during the 20 h experiment, and V_{un} is the average corrosion rate obtained during the 15 mins pre-corrosion, as indicated in Figure 5.

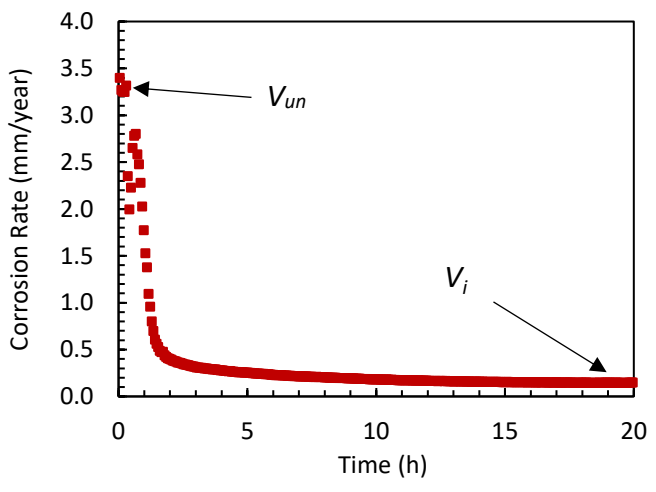


Figure 5: Corrosion rate vs time for X65 carbon steel exposed to a CO₂-saturated 1 wt.% NaCl brine solution in the presence of 100 μM BAC-C₁₆; inhibitor addition was performed after 15 minutes of pre-corrosion.

A series of RCE experiments such as the one depicted in Figure 5 were performed across a broad range of BAC-C₁₂ and BAC-C₁₆ concentrations. Figure 6 summarizes the corrosion inhibition performance extracted from numerous RCE experiments for both BAC-C₁₂ and BAC-C₁₆ as single components. The data is plotted as surface coverage (determined using Eq. 1) vs concentration, and a trend line is established using the Langmuir isotherm model, shown in Eq. 2:

$$\theta = \frac{\theta_{max} K_{ads}[CI]}{1 + K_{ads}[CI]}$$
 Eq. 2

where K_{ads} is the adsorption equilibrium constant (μ M⁻¹), [CI] is the concentration of BAC-C₁₂ or BAC-C₁₆ (μ M) and θ_{max} is the maximum surface coverage as [CI] $\rightarrow \infty$. The use of the Langmuir isotherm fit enables a continuous curve to be used to represent the relationship between the surface coverage of the inhibitor on the coupon and concentration.

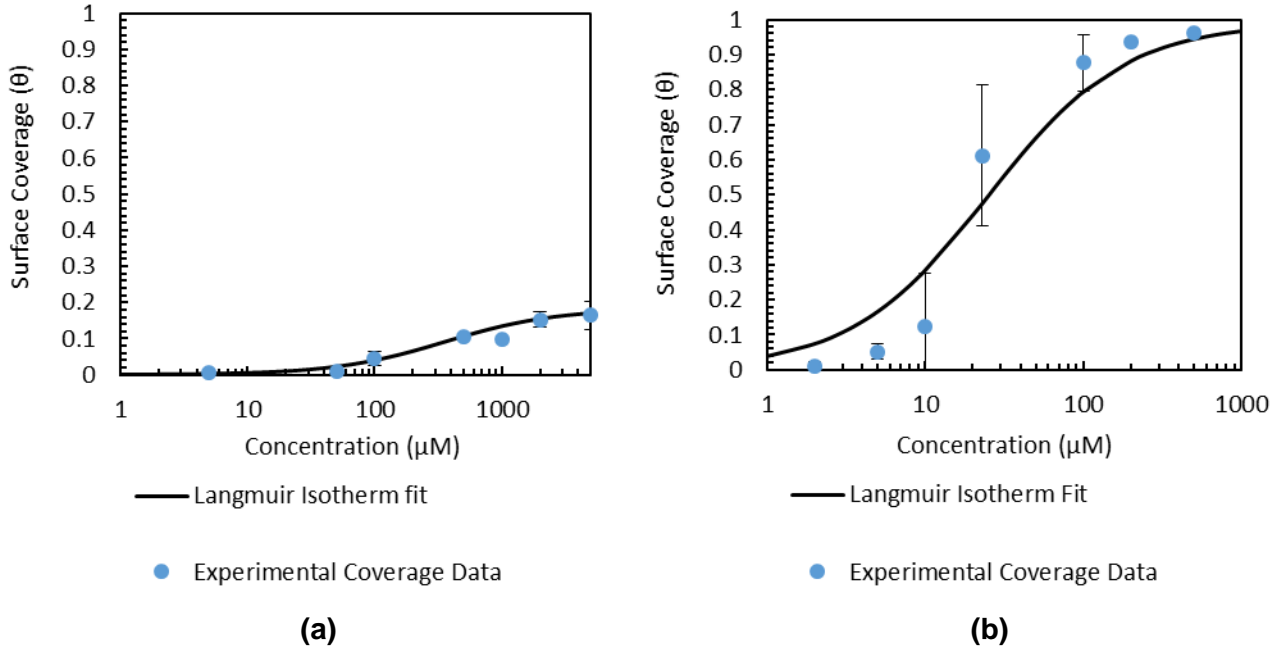


Figure 6: Corrosion inhibition performance and Langmuir Isotherm fit for (a) BAC-C₁₂ and (b) BAC-C₁₆ in a CO₂-saturated 1 wt.% NaCl brine at pH 4, 50°C and 1000 rpm

Figure 6(a) shows that the corrosion inhibition performance of BAC- C_{12} is very poor, even at a concentration of 5000 μ M with coverage only reaching 0.16 (16% efficiency). Conversely, BAC- C_{16} is very effective at inhibiting carbon steel corrosion in the 1 wt.% NaCl solution, reaching coverage values of over 0.96 (96% efficiency) beyond a concentration of 500 μ M.

Assuming inhibition from the two BAC surfactants is provided solely by their presence in the aqueous phase, it is possible to estimate the performance of each surfactant in the two-phase system by combining the coverage vs concentration data in Figure 6 with that of the partitioning responses for the toluenebrine system determined in Figure 1. The combined data and anticipated responses are provided in Figure 7, which correlates the agueous partitioning data with that of the corrosion inhibition performance curves. In Figure 7, the x-axis now corresponds to the total concentration of surfactant based on the bulk fluid. The upper graph represents the partitioning response from the model (solid black line) and the experimental HPLC-MS data is provided by the blue markers. The dashed yellow lines in the upper graphs of Figures 7(a) and (b) indicate the partitioning response that would be observed in the absence of micelle formation in the oil phase. The lower graphs within Figures 7(a) and (b) represent the inhibitor coverage response based on data from Figure 6, plotted as a function of total surfactant loading, and hence adjusted accordingly by accounting for the quantity of inhibitor partitioning into the aqueous phase. Again, the solid black lines represent the response that is observed practically based on the known distribution characteristics of each surfactant, whilst the yellow dashed lines indicate the unrestricted performance of the corrosion inhibitor if micelles were assumed to not form in the toluene phase i.e. the response if surfactant concentration in the aqueous phase does not plateau.

In Figure 7(a), the upper graph indicates that amount of BAC- C_{12} partitioning into the aqueous phase remains unrestricted, yet the lower graphs shows that the performance is poor, even at concentrations up to 5000 μ M based on the total fluid. Conversely, as shown in the lower graph of Figure 7(b) the performance of BAC- C_{16} , by comparison, is extremely good; at total fluid concentration of 800 μ M an efficiency of 90% is attained. However, this level of performance is only reached in the absence of micellization in the toluene phase. In reality, and in contrast to BAC- C_{12} , micelles composed of BAC- C_{16} form in the toluene phase, restricting the concentration of BAC- C_{16} in the aqueous phase is to ~10 μ M

(upper graphs of Figure 7(b)). The preferential partitioning into the toluene phase thereby limits the efficiency of BAC- C_{16} to ~30%, preventing the chemical from reaching its maximum inhibition performance.

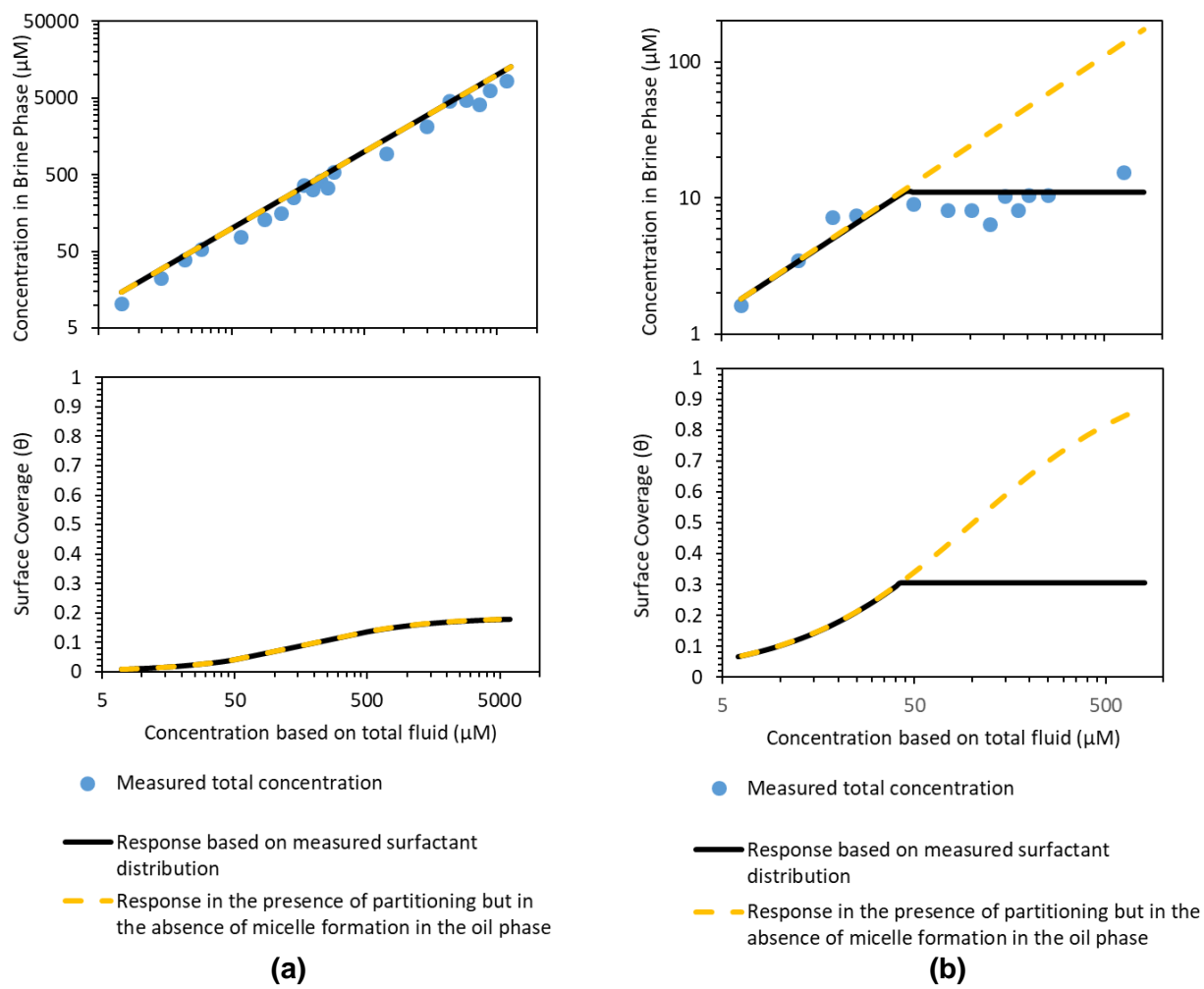


Figure 7: Comparison of partitioning behavior and corrosion inhibition performance for (a) BAC-C₁₂ and (b) BAC-C₁₆ in 1 wt.% NaCl brine at pH 4, 50°C and 1000 rpm. Partitioning tests were performed with a 50-50 mixture of brine and toluene.

Influence of Mixed Component Partitioning on Corrosion Inhibition Performance

The performance of BAC- C_{12} and BAC- C_{16} are contrasting. When added as single components, the two surfactants form micelles in opposing phases, and both exhibit markedly different levels of corrosion inhibition performance. Whilst BAC- C_{12} gives a preferable partitioning response by preferentially distributing into the brine phase, its corrosion inhibition performance is relatively poor, even at high concentrations of 5000 μ M. Conversely, BAC- C_{16} exhibits an unfavorable partitioning response, distributing preferentially into the toluene phase, yet its maximum inhibition potential is very high, though this cannot be realized due to restrictions in the aqueous phase concentration.

This poses the question as to whether a mixture combination of both surfactants is conducive to a more favorable overall response i.e. preferential distribution into the aqueous phase *and* improved performance from the distributed surfactant mixture.

Figure 4, shown previously, illustrated that the ratio BAC-C₁₂:BAC-C₁₆ can be adjusted to enable both BAC-C₁₂ and BAC-C₁₆ to preferentially partition into the aqueous phase. In terms of the evolution of the surfactant chemistry in the aqueous phase as a function of total surfactant loading beyond micelle

formation, this behavior is more complex. Figure 8 illustrates how the composition of the aqueous phase varies as a function of total concentration, ultimately converging towards the molar ratio of that added to the total fluid (i.e. 4:1).

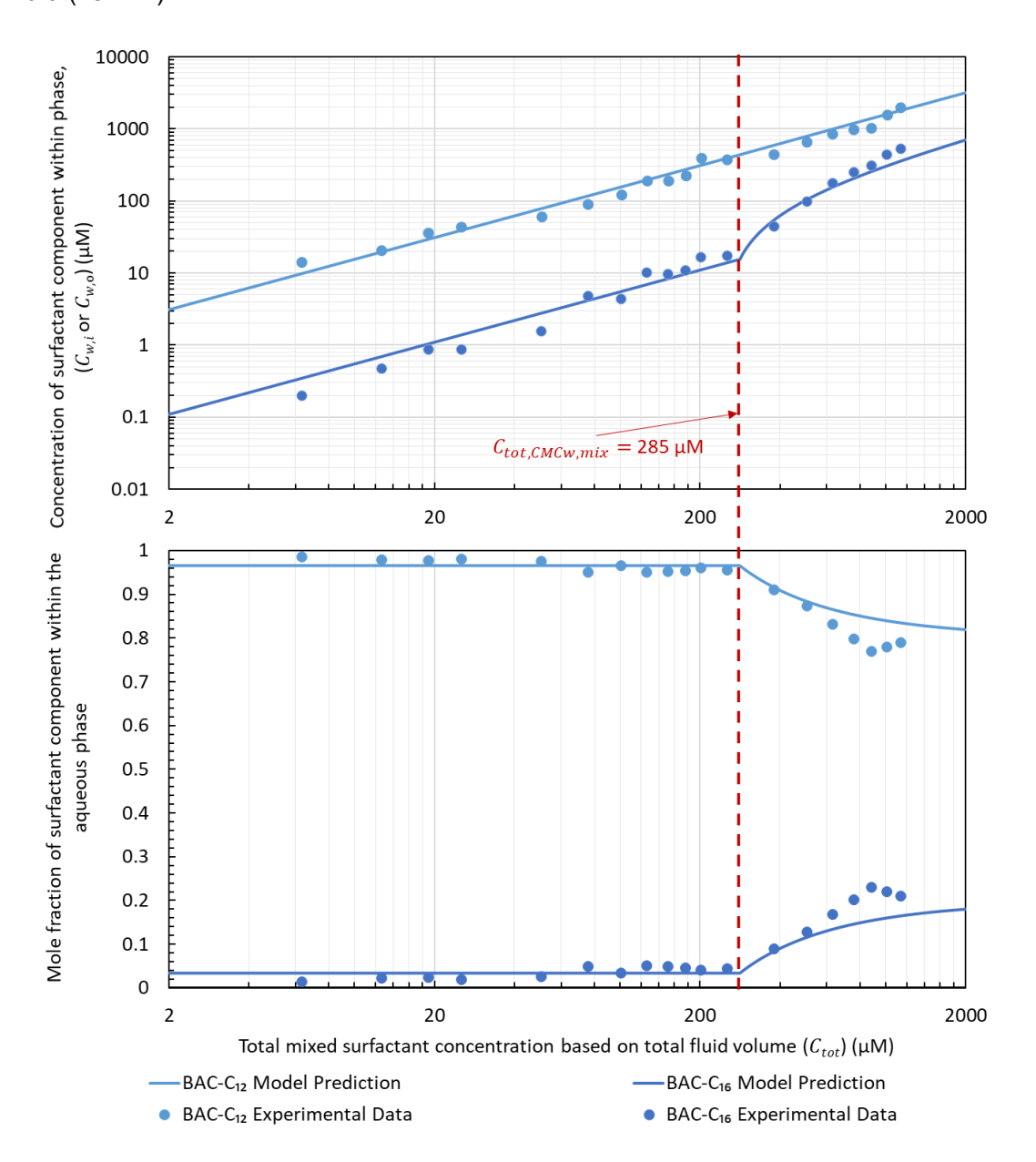


Figure 8: Variation in BAC- C_{12} and BAC- C_{16} surfactant concentration and composition of the aqueous phase as a function of total surfactant loading, predicted by distribution model for a 50-50 toluene-1 wt.% brine system at surfactant mixture molar ratio of 4:1 for BAC- C_{12} to BAC- C_{16}

As shown in Figure 9, and similarly to Figure 6, an isotherm model can be constructed based on the corrosion inhibition performance of the BAC- C_{12} /BAC- C_{16} mixture. It should be noted that in order to develop an appropriate isotherm response that can be correlated to the mixture partitioning behavior, corrosion experiments conducted at total mixture concentrations exceeding the aqueous CMC of 285 μ M were conducted using a molar ratio of BAC- C_{12} to BAC- C_{16} consistent with that shown in Figure 8. For example, for a total concentration of 1000 μ M, the ratio of BAC- C_{12} to BAC- C_{16} was 0.84:0.16.

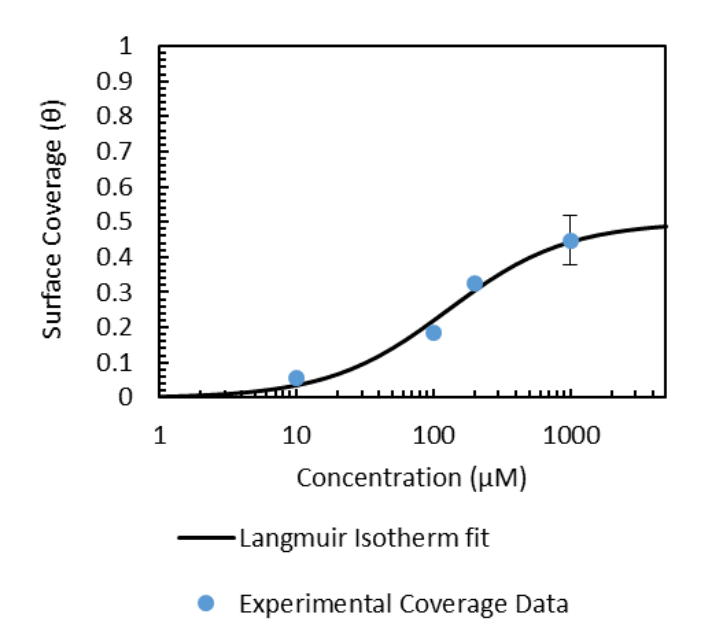


Figure 9: Corrosion inhibition performance and Langmuir Isotherm fit for BAC-C₁₂ and BAC-C₁₆ mixture in a CO₂-saturated 1 wt.% NaCl brine at pH 4, 50°C and 1000 rpm; molar composition of BAC-C₁₂ to BAC-C₁₆ matches those shown in Figure 8 for the same total concentration.

Figure 10 combines the isotherm model from Figure 9 with the total surfactant mixture partitioning behavior determined from Figure 8. Figure 10 illustrates a preferable distribution response of the surfactant into the aqueous phase, enabling the mixture to achieve its maximum corrosion inhibition potential. Despite the maximum inhibition efficiency of the mixture reaching only 50% (i.e. θ =0.5), the level of protection exceeds that of BAC-C₁₂ (20%) and BAC-C₁₆ (30%) applied individually when their respective distribution responses are considered.

Figure 11 compares the efficiency response of the pure BAC surfactants compared to that of the BAC- C_{12} /BAC- C_{16} mixture when accounting for the influence of partitioning on the concentration within the aqueous phase. Whilst BAC- C_{16} proved to be the most efficient chemistry, the preferential partitioning and micellization in the aqueous phase limits it maximum performance to below 30% (coverage of 0.3). Conversely, whilst the quantity of BAC- C_{12} that can partitioning to the aqueous phase remains unrestricted due to micellization in the aqueous phase, it is a relatively poor inhibitor resulting in a maximum efficiency of 16% (θ =0.16). When considering the BAC- C_{12} /BAC- C_{16} mixture, the maximum achievable efficiency is the highest, as the inhibition performance is superior to that of BAC- C_{12} and, unlike the BAC- C_{16} , the mixture concentration is unrestricted in the aqueous phase.

The results clearly demonstrate the synergistic effects associated with the different chain length molecules in this homologous series, demonstrating how they can work together to yield a favorable partitioning response and improve corrosion inhibition performance in the presence of an oil phase. It also highlights the importance of components perceived to be 'inactive' if assessed individually and purely from their ability to suppress corrosion.

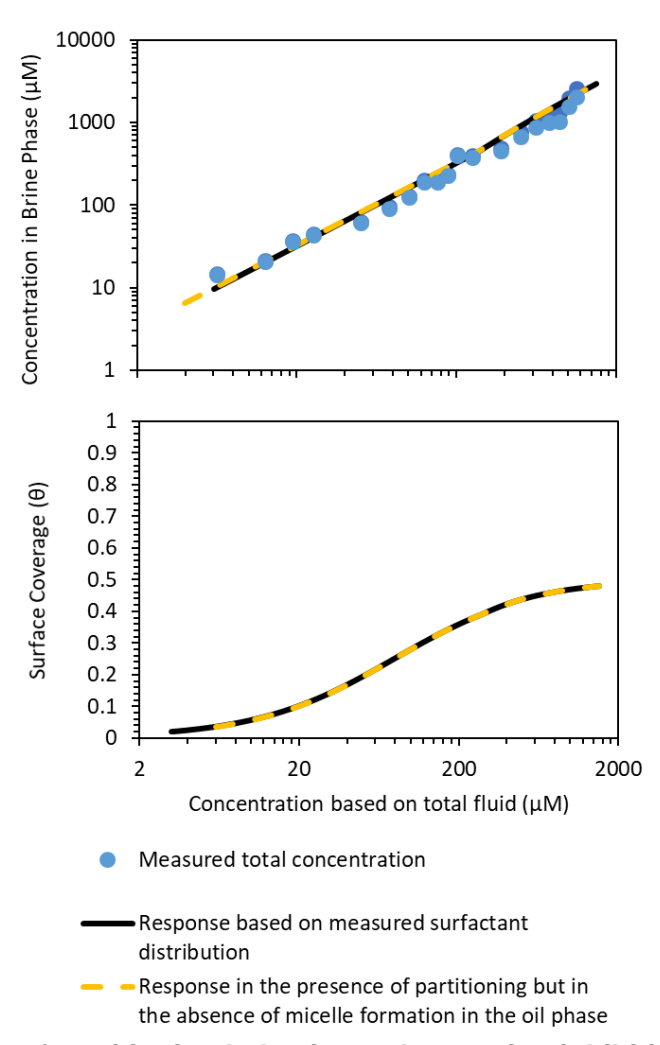


Figure 10: Comparison of partitioning behavior and corrosion inhibition performance for a 4:1 mixture of BAC-C₁₂ to BAC-C₁₆ (based on total fluid) in 1 wt.% NaCl brine at pH 4, 50°C and 1000 rpm. Partitioning tests were performed with a 50-50 mixture of brine and toluene.

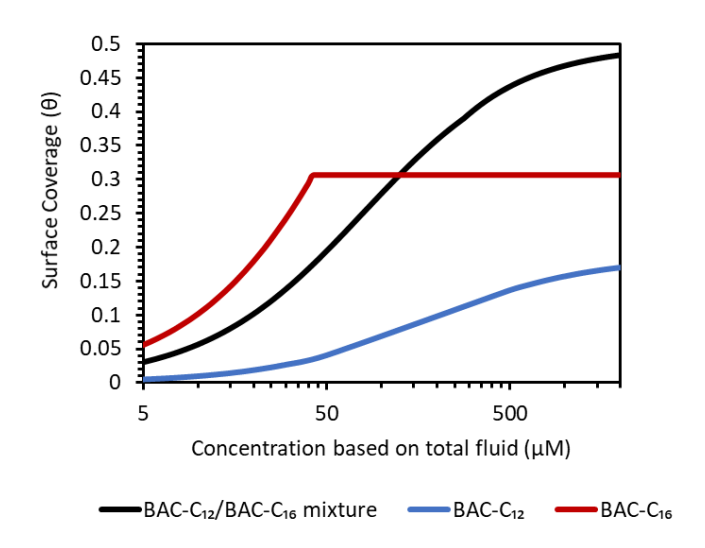


Figure 11: Comparison of pure BAC-C₁₂, pure BAC-C₁₆, and BAC-C₁₂/BAC-C₁₆ mixture as a function of concentration based on total fluid when accounting for the partitioning response.

CONCLUSIONS

In Part 1 of this two-part paper, a predictive model for multi-component partitioning was developed based on knowledge of individual component micellization and partitioning characteristics. In this paper, the model's validity was assessed through comparison with experimental partitioning data for an 1 wt.% NaCl brine:toluene system containing mixtures of benzylammonium chloride corrosion inhibitors (BAC- C_{12} and BAC- C_{16}).

The model is shown to provide an accurate assessment of each surfactant component's distribution response between brine and toluene, capturing the characteristics and location of the 'break-point' where the distribution response of each surfactant changes with increasing surfactant loading.

The implications of partitioning on corrosion inhibition performance of BAC- C_{12} and BAC- C_{16} were assessed when each surfactant was used in isolation. Despite BAC- C_{12} preferentially distributing into the brine phase, its maximum corrosion inhibition performance was low (20%). Conversely, BAC- C_{16} was capable of a maximum efficiency of >90%, yet its preferential distribution into the toluene phase results in the inhibition performance being restricted to 30%.

It was shown that a combination of BAC-C₁₂ and BAC-C₁₆ in the ratio 4:1 based on total fluid resulted in both a favorable distribution response (i.e. micellization in the aqueous phase), and superior corrosion inhibition performance compare to that achieved by each surfactant used in isolation when partitioning effects are considered.

Whilst the maximum achieved efficiency from the mixture was only 50%, the work demonstrates the synergistic effects associated with the different chain length molecules in this homologous series, demonstrating how they can work together to yield a favorable partitioning response and improve corrosion inhibition performance in the presence of an oil phase.

The paper opens up the opportunity to explore the potential of introducing additional surfactants with a view to 'tuning' mixtures to provide chemical blends optimized for performance and resilience to changes in environmental conditions such as salinity.

REFERENCES

- 1. R. Barker, J. Owen, R.C. Woollam, Y. Hayagheib, R. Bhamji, J. Williams, W.H. Durnie, M.C. Folena, A. Abdelmagid, and H. Farhat. *Correlating physical chemistry with interfacial properties: Effect of salinity on the partitioning, distribution and performance of a quaternary amine corrosion inhibitor.* in *AMPP Annual Conference+ Expo.* 2023. OnePetro.
- 2. Y. Zhu and M.L. Free, Experimental investigation and modeling of the performance of pure and mixed surfactant inhibitors: partitioning and distribution in water-oil environments. 2015. **162**(14): p. C702.
- 3. P. Alaei, B.P. Binks, P.D. Fletcher, I.E. Salama, and D.I. Horsup. *Surfactant properties of Alkylbenzyldimethylammonium chloride oilfield corrosion inhibitors*. in *NACE CORROSION*. 2013. NACE.